ELSEVIER

Journal of Alloys and Compounds 229 (1995) 216–222

Journal of ALLOYS AND COMPOUNDS

Ruddlesden–Popper zirconium sulfides—a novel preparation method and characterization of electronic structure

J. Yan[a], M. Greenblatt[a,*], A. Sahiner[b], D. Sills[b], M. Croft[b]

[a]*Department of Chemistry, Rutgers—The State University of New Jersey, Piscataway, NJ 08855-0939, USA*
[b]*Department of Physics, Rutgers—The State University of New Jersey, Piscataway, NJ 08855-0939, USA*

Received 16 January 1995; in final form 8 March 1995

Abstract

Barium zirconium sulfides, Ba_2ZrS_4 and $Ba_3Zr_2S_7$, were prepared by a novel precursor method. Ba_2ZrS_4 forms in the K_2NiF_4-type tetragonal ($I4/mmm$) structure with $a = 4.8379(5)$ Å and $c = 15.916(2)$ Å. $Ba_3Zr_2S_7$ forms in a distorted variant of the $Ba_3Zr_2O_7$ Ruddlesden–Popper-type orthorhombic ($Cccm$) structure with $a = 7.067(1)$ Å, $b = 25.557(4)$ Å and $c = 7.059(1)$ Å. Four probe electrical resistivity measurements show that the $Ba_{n+1}Zr_nS_{2n+1}$ ($n = 1, 2, \infty$) phases are semiconducting. The conductivity increases with increasing n. Seebeck measurements show that the majority charge carriers are holes. X-Ray absorption spectroscopy (XAS) measurements probing the electronic structure of these materials as viewed from the S and Zr sites are also discussed.

Keywords: Ruddlesden–Popper zirconium sulfides; Electronic structure

1. Introduction

A rich variety of oxides classified as Ruddlesden–Popper (RP) phases are described as intergrowth structures having the general formula $(AO)(AMO_3)_n$ [1,2]. In this formula, A is usually a rare earth, alkaline earth or an alkali metal ion and M can be a 3d or 4d transition metal ion. The structure is made up of n AMO_3 perovskite layers stacked between rock-salt-like AO layers along the crystallographic c axis. This structural arrangement imparts the materials with anisotropic properties. In La_2NiO_4 ($n = 1$ RP phase), for example, the conductivity along the basal plane is two orders of magnitude higher than along the [001] direction [3].

However, the literature on the corresponding RP chalcogenides is limited. Up to the present, $AS(ABS_3)_n$ RP phases have been reported only for A = Ba and B = Zr and Hf [4–7]. This finding is attributed to the participation of the nd electrons of the chalcogens in covalent bonding, and therefore only the most electropositive transition metals can form isostructural compounds with the oxides [8]. In this paper, a novel synthetic method for the synthesis of Ba_2ZrS_4 (214) and $Ba_3Zr_2S_7$ (327) is reported and these two phases together with the relevant perovskite-type $BaZrS_3$ (113) are characterized.

2. Novel synthetic method

The preparation of single phase Ba_2ZrS_4 in our laboratory using conventional solid state techniques, starting from stoichiometric amounts of BaS, Zr and S, was unsuccessful. CS_2/N_2 is a widely used sulfurization agent for the preparation of ternary chalcogenides [9,10] and we have attempted to use this mixture for the preparation of RP chalcogenides from oxides. The starting materials $BaCO_3$ (Aldrich, 99.98%) and $BaZrO_3$ (AESAR, 99%) in a 1:1 molar ratio were thoroughly mixed in an agate mortar and pressed into pellets. The pellets were placed in a tube furnace where CS_2 in N_2 carrier gas maintained a sulfurizing atmosphere at 750, 800 and 900°C respectively for several days. The powder X-ray diffraction (PXD)

* Corresponding author.

SSDI 0925-8388(95)01678-3

profiles show that perovskite-type $BaZrS_3$ and rock-salt-like BaS formed at 750°C; as the temperature was increased, the intensity of the peaks associated with BaS decreased, and the desired Ba_2ZrS_4 gradually formed. After the specimen was heated at 900°C for 3 days, the peaks due to BaS eventually disappeared and the peaks of Ba_2ZrS_4 became more intense and sharper, but the product was not monophasic; PXD showed evidence of $Ba_3Zr_2S_7$ impurity.

Although single phase Ba_2ZrS_4 could not be prepared by this approach, the mechanism of RP phase formation was suggested: as the RP phase is an intergrowth structure of perovskite layers stacked between rock-salt-like layers along the crystallographic c axis, the building blocks of perovskite $BaZrS_3$ and rock-salt BaS are required to form RP phases.

Perovskite-type dark brown $BaZrS_3$ was synthesized by sulfurizing $BaZrO_3$ with CS_2/N_2 at 900°C for 2 days. The PXD pattern of the product is in good agreement with the JCPDS file of $BaZrS_3$.

Based on our hypothesis of the mechanism of RP formation, single phases of Ba_2ZrS_4 and $Ba_3Zr_2S_7$ were prepared as follows. Stoichiometric amounts of $BaZrS_3$ and BaS were thoroughly mixed in an agate mortar and pelletized. The pellets were then sealed in quartz tubes and heated at a rate of 0.3°C min^{-1} to 1100°C and kept at that temperature for 30 h. The samples were then quenched to room temperature in air.

Figs. 1 and 2 show the X-ray diffraction patterns of Ba_2ZrS_4 and $Ba_3Zr_2S_7$ indexed in the tetragonal and orthorhombic system respectively. Least-squares refinement of the observed data is reported in Tables 1 and 2. The lattice parameters of Ba_2ZrS_4 obtained here are significantly different from those reported for

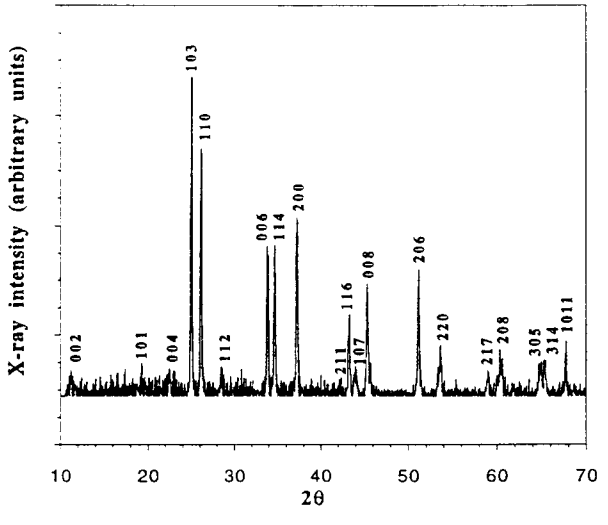

Fig. 1. X-Ray diffraction pattern of Ba_2ZrS_4.

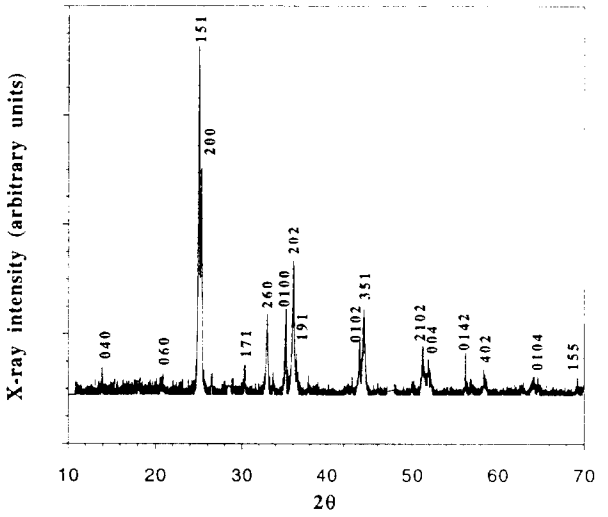

Fig. 2. X-Ray diffraction pattern of $Ba_3Zr_2S_7$.

Table 1
Powder X-ray diffraction data of Ba_2ZrS_4 (space group, $I4/mmm$; $a = 4.8379(5)$ Å; $c = 15.916(2)$ Å; $Z = 2$)

h	k	l	2θ	d_{obs}[a]	d_{cal}	I/I_0
0	0	2	11.10	7.966	7.967	4
1	0	1	19.17	4.626	4.629	4
0	0	4	22.33	3.978	3.979	7
1	0	3	24.90	3.573	3.575	100
1	1	0	26.03	3.420	3.421	78
1	1	2	28.38	3.143	3.143	4
0	0	6	33.75	2.654	2.653	45
1	1	4	34.56	2.594	2.594	37
2	0	0	37.12	2.420	2.419	49
2	1	1	42.10	2.144	2.144	2
1	1	6	43.12	2.096	2.092	21
1	0	7	43.97	2.058	2.058	5
0	0	8	45.57	1.989	1.990	27
2	0	6	51.04	1.788	1.787	28
2	2	0	53.54	1.710	1.710	12
2	1	7	58.90	1.567	1.567	5
2	0	8	60.20	1.536	1.537	6
3	0	5	64.75	1.439	1.439	7
1	0	11	67.51	1.386	1.386	7

[a] The error in d_{obs} is ±0.001 Å.

an impure phase of Ba_2ZrS_4 obtained by heating BaS + S + Zr in stoichiometric quantities at 1350°C [4].

Our attempt to prepare the $n = 3$ ($Ba_4Zr_3S_{10}$) compound as a single phase was unsuccessful. The final product with a ratio of $BaZrS_3/BaS = 3:1$ is always a mixture of $n = 3$, 2 and $n = \infty$ phases. This might be due to the fact that the $n = 3$ phase is thermodynamically metastable and the formation window is quite narrow. However, attempts to synthesize higher members of this family are continuing in our laboratory.

Table 2
Powder X-ray diffraction data of $Ba_3Zr_2S_7$ (space group, *Cccm*; $a = 7.067(1)$ Å; $b = 25.557(4)$ Å; $c = 7.059(1)$ Å; $Z = 4$)

h	k	l	2θ	d_{obs}[a]	d_{cal}	I/I_0
0	4	0	13.85	6.390	6.389	8
0	6	0	20.81	4.265	4.260	5
1	5	1	24.90	3.574	3.572	100
2	0	0	25.19	3.533	3.533	66
1	7	1	30.29	2.948	2.947	9
2	6	0	32.90	2.720	2.720	21
0	10	0	35.10	2.555	2.556	26
2	0	2	35.93	2.498	2.497	37
1	9	1	36.35	2.470	2.469	12
3	5	1	44.22	2.047	2.047	23
2	10	2	51.10	1.786	1.786	14
0	0	4	51.76	1.765	1.765	9
3	9	1	52.04	1.756	1.756	6
0	14	2	56.73	1.622	1.622	5
2	1	22	56.78	1.620	1.620	4
4	0	2	58.36	1.580	1.580	4
0	10	4	64.07	1.452	1.452	4
1	17	1	64.62	1.441	1.442	3
1	5	5	70.42	1.336	1.336	3
1	17	3	76.32	1.247	1.247	5

[a] The error in d_{obs} is ±0.001 Å.

3. Characterizations

3.1. Composition determination

The barium and zirconium contents were determined by a gravimetric technique and the sulfur content was determined as the difference. About 0.4000 g of a sample was dissolved in hot dilute nitric acid (20%); after effervescence of H_2S, a clear solution formed. The solution was cooled to room temperature, and phenylarsonic acid ($C_6H_5AsO_3H_2$) was added dropwise until no further white precipitate (zirconium phenylarsonate) was formed. After the precipitate of zirconium phenylarsonate had been separated by filtration, Na_2SO_4 (1 M) solution was added to the filtrate to precipitate all the Ba ions as $BaSO_4$. Zirconium phenylarsonate and $BaSO_4$ were then ignited at 1100°C for 24 h in alumina crucibles to yield ZrO_2 [11] and $BaSO_4$ respectively. As shown in Table 3, there is a small sulfur deficiency for all three phases, but the Ba and Zr contents are nearly stoichiometric within experimental error.

3.2. Transport property measurements

The electrical resistivities of $BaZrS_3$, Ba_2ZrS_4 and $Ba_3Zr_2S_7$ were measured by a standard four probe technique in a DE202 cryostat (APD Cryogenics) from room temperature to 30 K (Fig. 3). Qualitative Seebeck measurements show that the primary charge carriers are holes in all three phases.

Table 3
Chemical analysis of three RP zirconium chalcogenides

Element	Ba (wt.%)	Zr (wt.%)	S (wt.%)
$BaZrS_3$			
Experimental	42.1(2)[a]	28.3(2)	28.5(2)
Calculated	42.3	28.1	29.6
Ba_2ZrS_4			
Experimental	55.4(2)	18.3(2)	25.0(2)
Calculated	55.6	18.4	26.0
$Ba_3Zr_2S_7$			
Experimental	50.2(2)	22.4(2)	26.5(2)
Calculated	50.3	22.3	27.4

[a] Numerical values in parentheses are the standard deviations.

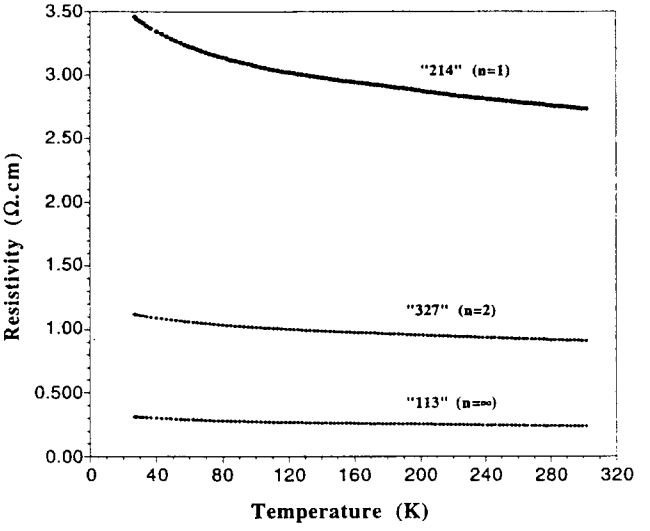

Fig. 3. Resistivity vs. temperature of "113", "214" and "327" phases.

3.3. X-Ray absorption spectroscopy (XAS) measurements

The XAS measurements on the polycrystalline Ba–Zr–S materials were performed in the total electron yield mode on beam line X-19A at the Brookhaven National Synchrotron Light Source. A focused beam and a double crystal Si(110) monochromator were used.

4. Results and discussion

Although exact energy band calculations have not been performed on the RP chalcogenides, some general comments can be made on the basis of the band diagram of the corresponding perovskite-related oxides (ABO_3) proposed by Goodenough and Longo [12]. The valence band is usually built up of the 3s and 3p orbitals of sulfur and the (n + 1)s and (n + 1)p orbitals of the transition metals. As shown in Fig. 3, all

of these phases are semiconducting with relatively high room temperature conductivities; the electrical resistivity decreases over the whole temperature range measured as the number of perovskite layers (n) increases. This behavior is similar to that observed in RP nickel and vanadium oxides [13–18] and may be due to the enhancement of phase space for electronic correlations.

The $\ln\rho$ vs. $1/T$ plots for all three phases show non-linear behavior over the whole temperature range of measurement. However, the apparent activation energies (E_a) can be obtained from the data between 180 and 300 K since $\ln\rho$ vs. $1/T$ behaves roughly linearly in this temperature range. As shown in Table 4, the activation energies for all three phases are very low (approximately 10^{-3} eV) and, although E_a is highest for $BaZrS_3$ ($n = \infty$), the trend is not exactly in line with the trend in resistivity (Fig. 3). This result may be attributed to the differences in the pre-exponential factors (i.e. ρ_0 in $\rho = \rho_0 e^{-E_a/RT}$) for different phases, which depend on the concentration of charge carriers in the system.

A better linear fit of $\ln\rho$ vs. $T^{-1/4}$ than $1/T$ is obtained as illustrated in Fig. 4. This correlation suggests a phonon-assisted variable-range hopping mechanism for the electrical conductivity [19,20].

Table 4
Resistivity and apparent activation energy for $Ba_{n+1}Zr_nS_{2n+1}$ ($n = 1, 2, \infty$)

Compound	$\rho_{(300\,K)}$ (Ω cm)[a]	E_a ($\times 10^{-3}$ eV)[b]
$BaZrS_3$	0.24	1.38
$Ba_3Zr_2S_7$	0.91	0.94
Ba_2ZrS_4	2.73	1.05

[a] The error in the resistivity measurement is ±20%.
[b] Derived from the temperature range of 180–300 K; the error is ±0.01 eV.

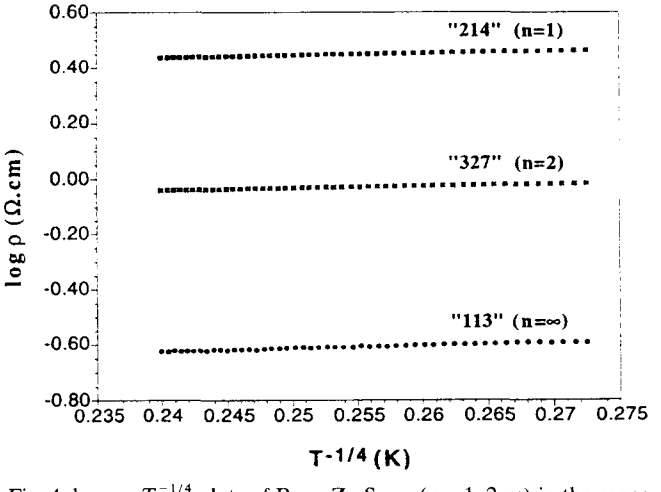

Fig. 4. $\ln\rho$ vs. $T^{-1/4}$ plots of $Ba_{n+1}Zr_nS_{2n+1}$ ($n = 1, 2, \infty$) in the range $180 < T < 300$ K.

The S–K edge provides two indicators of the S charge-state/p-orbital occupation: the near edge "white line" (WL) feature and the chemical shift of the edge [21]. The elemental S–K edge (see Fig. 5, top) is dominated by the intense WL feature caused by dipole-allowed S 1s to S 3p transitions. The intensity of this WL feature scales with the number of S 3p orbital holes. The dramatic depression of the S–K–WL feature in $BaZrS_3$ (see Fig. 5, top) reflects the filling of S 3p orbital holes in the compound via charge transfer from the metal Ba and Zr sites.

A leitmotif in core level spectroscopy (both photon and electron induced) is the chemical shift of the spectra to higher (lower) energy when electronic charge is transferred out of (into) an atom's orbitals [21,22]. In Fig. 5 (top), there is a clear downward shift in the S–K edge spectra of $BaZrS_3$ relative to elemental S. Thus, as in the case of the WL strength, the chemical shift supports the transfer of electronic charge to the S sites.

In Fig. 5 (bottom), the S–K edges of $BaZrS_3$, $Ba_3Zr_2S_7$ and Ba_2ZrS_4 are displayed on the same energy scale as that of elemental S (in the top figure) and their downward energy shifts are underscored by

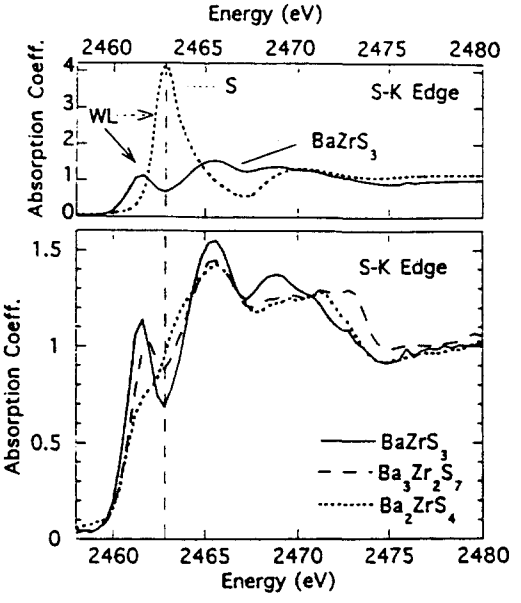

Fig. 5. Top. A comparison of the S–K edge spectra for elemental S and $BaZrS_3$. The "white line" (WL) features of both spectra are labeled and correspond to dipole-allowed S 1s to S 3p transitions. The dramatic decrease in the WL spectral intensity in the compound is evidence of the filling of S 3p orbital holes in the compound via charge transfer from the metal sites. The shift of the S–K edge towards lower energy in the compound (relative to the element) further supports the increase in electronic charge on the compound S site relative to the element. Bottom. The overlaid S–K edge spectra of $BaZrS_3$ (113), $Ba_3Zr_2S_7$ (327) and Ba_2ZrS_4 (214). Note the systematic decrease in the WL feature in these compounds in the sequence 113 to 327 to 214. The broken line indicates the elemental S WL energy.

the broken vertical line marking the pure S WL energy. From the figure it is clear that the pre-edge WL feature decreases in intensity in the 113 to 327 to 214 sequence of materials. Thus, since we associate this WL intensity with the S p hole count, this spectral intensity loss reflects a decrease in the S p hole count in this sequence of compounds.

It is important to recall that the resistivity measurements show decreasing conductivity in the 113 to 327 to 214 sequence of materials (Fig. 3) and, moreover, that the Seebeck coefficient indicates hole-type charge carriers. These results correlate well with our S–K edge XAS results. Specifically, the presence of S p holes is consistent with the Seebeck measurement and the increasing number of S p holes correlates with the increasing conductivity.

In studies of the O–K edge of Cu–O-based high T_c materials, the presence of similar pre-edge features has been interpreted in terms of O p hole states just above E_F. In these systems, the intensity increase of these pre-edge features was argued to be the above E_F extension of O p states which extended below the Fermi energy [23–25]; of course, these O p hole states provide the conductivity and support the superconductivity in these Cu–O systems. It would appear that the situation in the Ba–Zr–S Ruddlesden–Popper materials is similar to that in the high T_c cuprates, namely there is XAS evidence for hole states primarily associated with sulfur 3p orbitals and a correlation exists between the qualitative XAS estimate of the number of such holes and the conductivity.

Atomic-like 2p to 4d transitions endow the L_2 and L_3 edges of 4d row transition metals (like Zr) with extremely intense WL features. The strength and structure of these WL features convey information regarding the distribution of 4d states above the Fermi energy in compounds containing these metals. For example, in Fig. 6 (top), the Zr L_3 spectrum of the perovskite $BaZrO_3$ clearly shows the 4d orbital octahedral crystal field (CF) splitting through the sharp splitting of the WL into A and B features. (The Zr L_2 spectrum of the same compound manifests the same splitting, but with a somewhat different A:B intensity ratio. The choice to display the L_3 spectrum here is based on its superior signal-to-noise ratio.) This splitting by the CF of the 4d $L_{2,3}$ spectra has been reported previously in the literature [26]. The magnitude of the final state CF splitting is about 3.7 eV (as indicated in the figure). To extract the initial state CF splitting, this value would have to be corrected for the absence of the core hole in the initial state. However, the relative comparison with the S-based materials (below) can proceed without such a correction.

The Zr L_2 spectra for the $BaZrS_3$, $Ba_3Zr_2S_7$ and Ba_2ZrS_4 compounds are shown in Fig. 6 (bottom). Comparison of the $BaZrX_3$ spectra for X=O (in the top figure) and X=S (in the bottom) underscores the dramatically smaller CF splitting of the Zr d orbitals in an S octahedron (1.5 eV) relative to that in an O octahedron (3.7 eV). This large change in electronic structure is not surprising in view of the fact that O^{2-} exerts a stronger crystal field than S^{2-} [27].

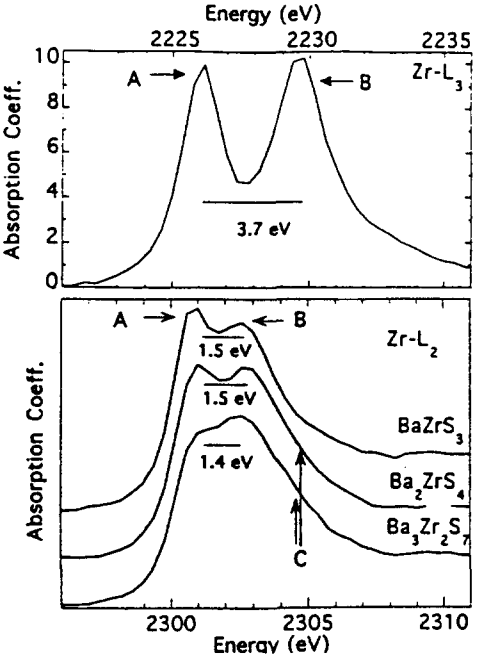

Fig. 6. Top. The Zr L_3 edge spectra of $BaZrO_3$ illustrating the sharp splitting of WL into t_{2g} and e_g related features labeled A and B respectively. The crystal field splitting of these final state features is about 3.7 eV. The excess Zr core hole in the final state would require a correction of this value to find the initial state t_{2g}–e_g splitting. Note that although the spectral intensities of the split states change from the Zr L_3 to the Zr L_2 edges, the splittings remain the same and hence comparison with the Zr L_2 spectra is appropriate. Bottom. The Zr L_2 edge spectra of $BaZrS_3$ (113), $Ba_3Zr_2S_7$ (327) and Ba_2ZrS_4 (214). Several points should be noted: the dramatic decrease in the crystal field (A–B) splitting in these S perovskite-based materials compared with the oxide perovskite above; the layered 327 and 214 materials exhibit a substantial high energy broadening (identified by C in the figure) relative to the 113 perovskite; the sharpness and relative intensity of the A feature decreases in the spectral sequence 113 to 327 to 214.

Comparison of the S-based compound spectra reveals two clear systematic changes. First, there is a broadening of the 214 and 327 spectra in the high energy range identified by C in the figure. Second, the A feature broadens and degrades in the 113 to 214 to 327 sequence. It is worth noting that the Zr site coordination is progressively less symmetric in this sequence; in the 113 material it is octahedral, in the 214 material the two apical S bonds are symmetrically dilated, and in the 327 material one of the apical S atoms bridges to another Ba site while the other is similar to that in the 113 compound [7]. Presumably, the high energy broadening (C) is related to the loss of pure octahedral symmetry. Similarly, the progressive

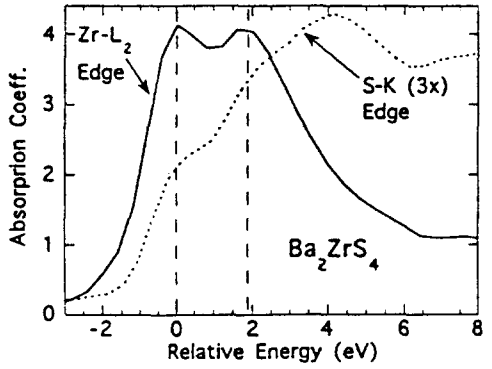

Fig. 7. The energy aligned and overlaid S–K (expanded by 3 ×) and Zr L_2 edge spectra of Ba_2ZrS_4. The intense Zr WL feature is due to Zr 2p to Zr 4d transitions and its splitting reflects the t_{2g}–e_g splitting of the Zr 4d final states. The weak bimodal features below the S–K edge exhibit a similar splitting (as emphasized by the broken vertical lines) suggesting an S p/Zr d hybridization.

reduction in the Zr site bonding symmetry in the 113 to 214 to 327 sequence is presumably responsible for the spreading in the low-lying Zr d states represented by feature A. Clearly, electronic structure calculations to address these issues are called for.

Close examination of the S–K spectrum of the 214 compound in Fig. 5 (bottom) reveals a second subtle shoulder below the main edge (near 2464 eV). With this in mind, two points should be noted: the Zr L_2 WL features were also bimodal and, in some 3d transition metal oxides, hybridization can lead to the observation of d state character in the O–K pre-edge spectral features [28]. The Zr L_2 and S–K (threefold expanded in amplitude) spectra for the 214 material are plotted in Fig. 7 on the same energy scale with their first features aligned. The broken lines indicate the similarity of the energy splitting of the features in the two spectra making the notion of a Zr d hybridization contribution to the S–K features plausible. The magnitude of such an effect in this compound (and perhaps the others) will require careful electronic structure and transition matrix element calculations.

5. Conclusions

Single phases of Ba_2ZrS_4 and $Ba_3Zr_2S_7$ were prepared from $BaZrS_3$ and BaS by solid state reaction methods. Together with the perovskite $BaZrS_3$, all these phases show a slight sulfur deficiency and p-type semiconducting behavior. The sulfur deficiency appears to be irreversible, as heating a sample of as-prepared $BaZrS_{3-\delta}$ ($\delta = 0.16$) in a sulfur atmosphere does not change the value of δ or the physical properties of the sample. Semiconducting and p-type behavior, as well as increasing electrical conductivity with increasing n in $Ba_{n+1}Zr_nS_{2n+1}$ ($n = 1, 2, \infty$), was observed. The S–K edge XAS measurements show evidence of S p orbital hole states; the number of these states increases with n, which therefore correlates with the electrical conductivity variation.

Finally, motivation and guidelines for electronic structure calculations are provided by the unoccupied state distributions of Zr d and S p character inferred from the Zr L_2 and S–K XAS results respectively.

Acknowledgments

We thank Dr. S.C. Chen and Dr. K.V. Ramanujachary for helpful discussions. This work was supported by the National Science Foundation Solid State Chemistry Grants DMR-90-19301 and DMR-93-14605.

References

[1] S.N. Ruddlesden and P. Popper, *Acta Crystallogr., 11* (1958) 54.
[2] S.N. Ruddlesden and P. Popper, *Acta Crystallogr., 10* (1957) 538.
[3] C.N.R. Rao, D.J. Buttery and J.M. Honig, *J. Solid State Chem., 51* (1984) 266.
[4] B.-H. Chen and B. Eichhorn, *Mater. Res. Bull., 26* (1991) 1035.
[5] B. Chen, B.W. Eichhorn and P.E. Fanwick, *Inorg. Chem., 31* (1991) 1788.
[6] B.-H. Chen, W. Wong-ng and B.W. Eichhorn, *J. Solid State Chem., 103* (1993) 75.
[7] M. Saeki, Y. Yajima and M. Onoda, *J. Solid State Chem., 92* (1991) 286.
[8] F. Jellink, in *International Review of Science, Inorganic Chemistry, London, 1972.*
[9] M. Saeki and M. Onoda, *Mater. Res. Bull., 25* (1990) 723.
[10] M. Saeki, H. Nozaki and M. Onada, *Mater. Res. Bull., 24* (1989) 851.
[11] R.A. Gardner, *Ph.D. Thesis*, Brown University, 1969.
[12] J.B. Goodenough and J.M. Longo, *Landolt-Bornstein, Group III*, Vol. 4a, Springer, Berlin, Heidelberg, 1970, Chapter 3, p. 131.
[13] R.A.M. Ram, L. Ganapathi, P. Ganguly and C.N.R. Rao, *J. Solid State Chem., 63* (1986) 139.
[14] V.F. Savchenko, L.S. Ivashkevich and I.Y. Lyubkina, *Russ. J. Inorg. Chem., 33* (1) (1988) 17.
[15] M. Itoh, M. Shikano, H. Kawaji and T. Nacamura, *Solid State Commun., 80* (8) (1991) 545.
[16] Z. Zhang, M. Greenblatt and J.B. Goodenough, *J. Solid State Chem., 108* (1994) 402.
[17] Z. Zhang and M. Greenblatt, *J. Solid State Chem.*, to be published.
[18] K. Sreedlar, M. McElfresh and J.M. Honig, *J. Solid State Chem., 110* (1994) 208.
[19] S. Li, K.V. Ramanujachary and M. Greenblatt, *Physica C, 166* (1990) 535.
[20] B. Dabrowski, D.G. Hinks, J.D. Jorgensen, R.K. Kalia, P. Vashishata, D.R. Richards, D.T. Marx and A.W. Mitchell, *Physica C, 156* (1988) 24.
[21] G. Huffman, S. Mitra, F. Huggins, N. Shah, S. Vaidya and F. Lu, *Energy Fuels, 5* (1991) 574.
[22] For a similar treatment of iodine p occupancy changes, see G.

Liang, A. Sahiner, M. Croft, W. Zu, X.-D. Xiang, D. Badresh, W. Li, J. Chen, J. Peng, A. Zettl and F. Lu, *Phys. Rev. B, 47* (1993) 1029, and references cited therein.

[23] C. Chen, F. Sette, Y. Ma, M. Hybersteen, S. Stechel, W. Foulks, M. Schuler, S.-W. Cheong, A. Cooper, L. Rupp, B. Battlogg, Y. Soo, Z. Ming, A. Krol and Y. Kao, *Phys. Rev. Lett., 66* (1991) 104.

[24] H. Eisaki, S. Uchida, T. Mizokawa, H. Nmatame, A. Fujimori, J. van Elp, P. Kupier, A. Sawatzky, S. Hosoya and H. Katayama-Yoshida, *Phys. Rev. B, 45* (1992) 12513.

[25] P. Kupier, J. van Elp, G.A. Sawatzky, A. Fujimuri, S. Hosoya and D.W. de Leeuw, *Phys. Rev. B, 44* (1991) 4570.

[26] G. George, W. Cleland, J. Enemark, B. Smith, C. Kipke, S. Roberts and S. Cramer, *J. Am. Chem. Soc., 112* (1990) 2541.

[27] J.E. Huheey, *Inorganic Chemistry*, Harper & Row, New York, 1983.

[28] F. deGroot, M. Grioni, J. Fuggle, J. Ghijsen, G.A. Sawatzky and H. Petersen, *Phys. Rev. B, 40* (1989) 5715.